CHARACTERIZATION OF ELECTROTHERMAL ACTUATORS AND ARRAYS FABRICATED IN A FOUR-LEVEL, PLANARIZED SURFACE-MICROMACHINED POLYCRYSTALLINE SILICON PROCESS

John H. Comtois*, M. Adrian Michalicek*, and Carole Craig Barron**
*U.S. Air Force Phillips Laboratory, KAFB, NM 87117
**U.S. Department of Energy, Sandia National Laboratories, KAFB, NM 87117

SUMMARY

This paper presents the results of tests performed on a variety of electrothermal microactuators and arrays of these actuators recently fabricated in the four-level planarized polycrystalline silicon (polysilicon) SUMMiT process at the U. S. Department of Energy's Sandia National Laboratories [1]. These results are intended to aid designers of thermally actuated mechanisms, and will apply to similar actuators made in other polysilicon MEMS processes. The measurements include force and deflection versus input power, maximum operating frequency, effects of long term operation, and ideal actuator and array geometries for different design criteria. A typical application in a stepper motor is shown to illustrate the utility of these actuators and arrays.

Keywords: microactuators, electrothermal, SUMMiT

ELECTROTHERMAL MICROACTUATORS

The basic device studied in this research is a single-material actuator which deflects at its tip by unequal thermal expansion of its constituent parts. A typical 'U' shaped electrothermal actuator is shown in Fig. 1. Current is passed through the actuator via the anchors, and the higher current density in the narrower 'hot' arm results in greater ohmic heating, causing it to expand more than the wider 'cold' arm. The arms are joined at the free end, which constrains the actuator tip to move laterally in an arcing motion towards the cold arm side [2,3]. Backwards deflection can be achieved by momentarily over-driving the hot arm which causes it to deform plastically, decreasing its overall length. The actuator then bends backwards past its initially fabricated position when the power is removed. The actuator can therefore deliver a static force, or it can be operated in the forward direction from its new starting position [4].

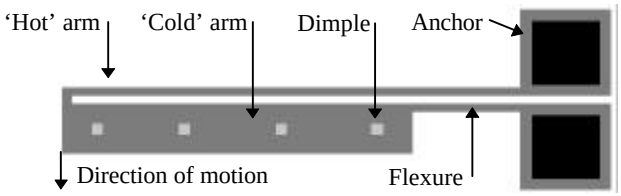

Figure 1. Schematic view of an electrothermal actuator.

This simple actuator can be fabricated in any MEMS process that includes at least one releasable, current carrying layer. A typical 200 μm long actuator is capable of 16 μm of deflection when unloaded, and can deliver up to 13 μN of force. Arrays of actuators allow the generation of many 10's of μN of force. Most importantly, these actuators operate in a current and voltage regime which is directly compatible with standard CMOS electronics, e.g. 0 to 14 volts at 0 to 5 mA, depending on the geometry and maximum deflection desired.

SUMMiT FABRICATION PROCESS

The devices presented in this paper were fabricated in the SUMMiT (Sandia Ultra-planar Multi-level MEMS Technology), through the SAMPLE (Sandia Agile MEMS Prototyping, Layout tools, and Education) service [5]. As in other surface-micromachining processes, the devices are formed in SUMMiT by the alternate deposition of structural polysilicon layers and sacrificial oxide layers, over a base nitride layer. These devices were etched in a 1:1 mix of HF:HCL and dried in supercritical carbon dioxide process.

The complexity of the micromachines which can be manufactured in a given process is a function of the number of independent layers of structural polysilicon the technology provides. Although the actuators presented in this paper require only one releasable structural layer, complex applications of them usually require more. Geared mechanisms, for example, require two independent levels (one to form the hubs and the other the moving gears), and reduction-geared mechanisms require three independent levels. Unique advantages of the SUMMiT process include one-micron feature sizes, planarization of the third polysilicon level, and the ability to make flanged gear hubs and electrical contacts to the substrate.

SINGLE ACTUATOR TESTS

This section reports the condensed results of tests performed on single actuators of 90 slightly different geometries. The variations are used to pinpoint the ideal geometry for applications requiring different deflections and forces. The actuators fall into 4 categories by overall length, and within those categories are variations of hot arm width, flexure length and the width of the gap between the two arms. All of the actuators are made of stacked Poly-1 and Poly-2 because the thicker polysilicon layer puts the overall device resistance into a range that makes it CMOS-compatible, i.e. a cold resistance in the range of 0.5 to 3 kilohms.

The actuators are instrumented to measure their output force at different deflections. The instrumentation consists of scales to measure deflection and bending beams of different widths for the actuators to press against, as shown in Fig. 2. Actuators with no load were tested for their deflection versus power characteristics, to determine which geometrical variations produced the largest deflection at the lowest input power. The actuators were tested by advancing the deflection in 1 ± 0.25 μm increments and recording the voltage and current. Each actuator was deflected until it showed the initial signs of back-bending, i.e. the loss of forward deflection due to plastic deformation of the hot arm. Table 1 lists the ideal dimensions to achieve the highest deflection at the lowest input power for unloaded or lightly loaded (<1μN) actuators of different lengths, and Fig. 3 shows their deflection versus input power responses.

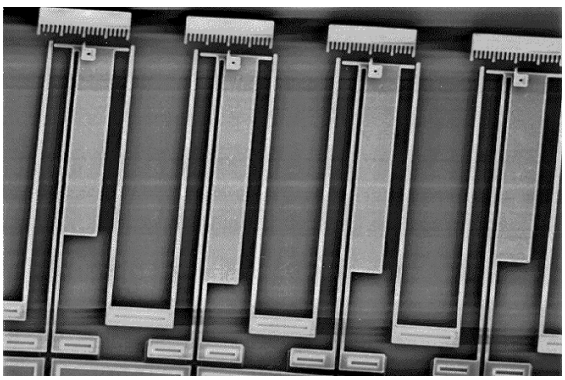

Figure 2. Four independent 150 μm long actuators, each instrumented with deflection scales and two test beams for measuring force in both forward and backward deflection.

Table 1. Ideal dimensions for unloaded or lightly loaded actuators. All dimensions are in microns.

Length	Hot arm width	Flexure length	Gap width
150	1	30	1.5
200	1.5	50	1.5
250	1.5	80	1.5
300	2	75	1.5

For unloaded or very lightly loaded actuators, it is generally best to use the thinnest possible hot arm. This lowers the power requirement. A longer flexure will deflect a micron or two more, but will also heat, resulting in a slight overall increase in power at each deflection setting. The 300 μm long actuators exhibited an oscillation caused by the hot arm bowing down and touching the substrate, which cools the arm causing it to shrink up out of contact again. This effect was also sometimes observed in the 250 μm long actuators, at higher deflections.

Measurements similar to those of unloaded deflection versus power were taken on identical actuators instrumented with force test beams, as shown in Fig. 2. Because hot arm oscillation affected the longest actuators, they were not tested for force. It turns out that the actuators that give the best deflection per input power performance when unloaded do not give the best power consumption performance when loaded. The results of these tests are summarized in Table 2, which lists the ideal dimensions for best overall power versus force characteristics for heavily loaded actuators. Interestingly, the actuators with the shortest flexures did better for delivering the most force despite the fact that a shorter flexure is harder to bend. The reason is that the longer flexures tend to bend into a shallow "S" shape instead of a simple curve, allowing the actuator tip to back away from the load beam.

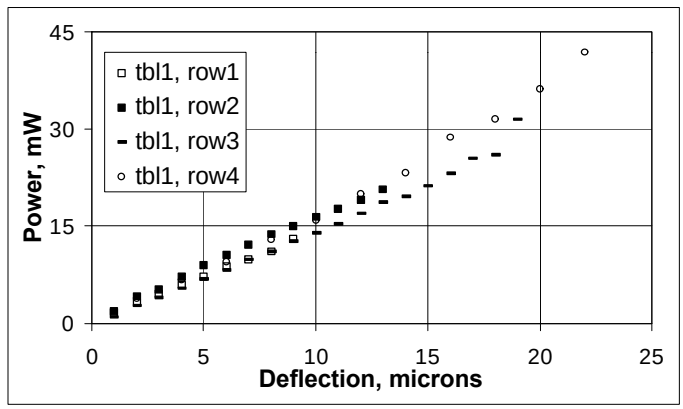

Figure 3. Deflection versus power for the actuators listed in Table 1. Maximum voltages applied to the 150, 200, 250, and 300 μm long actuators were 8.3, 9, 13, and 13.7 V respectively.

Table 2. Ideal dimensions for heavily loaded actuators, for best power versus force performance. Dimensions in microns.

Length	Hot arm width	Flexure length	Gap width
150	1.5	30	1.5
200	2	50	2
250	2.5	50	1.5

Table 3 lists the dimensions of the actuators that delivered the maximum force at any power. The highest forces were delivered by the actuator types with a wider hot arm and a larger gap between arms. The wider hot arm provides more expanding material, and a wider gap increases the leverage of the hot arm. However, a wider gap also decreases the overall deflection, so that route to higher forces leads to diminishing returns if higher deflections are also needed.

For all the actuator types, more force can be delivered at lower deflections, since the actuator must also bend its own flexure, which requires more force the farther it bends. Also, the hot arm delivers less force by bowing more out of line at higher deflections, thus pressing less on the tip of the actuator. Figure 4 shows the force versus input power for actuators listed in Tables 2 and 3.

In general a longer actuator will deflect farther when unloaded and will deliver more force, but the trend stops when the hot arm gets long enough to sag onto the substrate, which occurred regularly at 300 μm length. Dimples can be used to support the hot arm, but they still provide some heat loss area and add a stick-slip motion, which makes the deflection of the actuator less predictable. Longer actuators also require more power for the same force as a shorter one, so if both can deliver the same force it is best to use the smaller actuator.

The maximum operating frequency for these actuators is defined to be the square wave frequency at which the actuator no longer reaches the full deflection it achieves at the same peak voltage in DC operation. These actuators typically had a maximum frequency of between 0.4 and 1.6 kHz, with longer actuators having lower maximum frequencies. However, the actuators were still observed to have a useful deflection (2 μm) at much higher frequencies. For example, a 200 μm long actuator had a maximum frequency of 1.48 kHz for full deflection, but still showed about 2 μm of deflection at 13 kHz, which is useful for optical applications. The results of tests on actuators listed in Table 1 are summarized in Table 4.

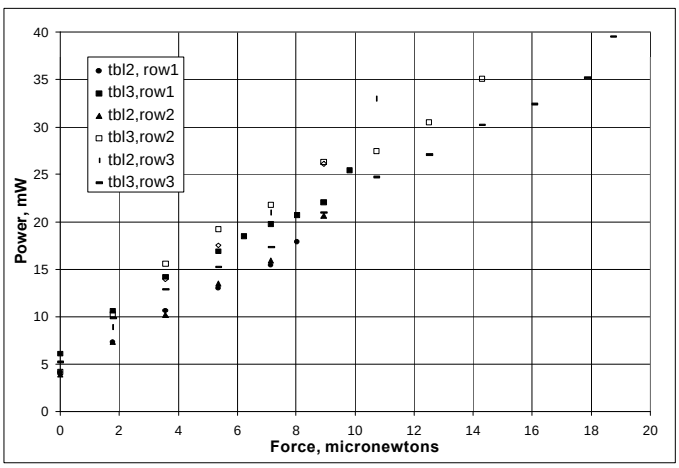

Figure 4. Force versus power for the actuator types listed in Tables 2 and 3.

Table 3. Dimensions of actuators that delivered the highest force at any power. All dimensions are in microns.

Length	Hot arm width	Flexure length	Gap width
150	2	30	2
200	2.5	65	2
250	3	75	2

Table 4. Operating frequency characteristics for unloaded actuators of different lengths.

Length & deflection tested, μm	Maximum frequency at full deflection	Frequency at ½ deflection	Frequency where motion stops
150, 7	1.57 kHz	7 kHz	24 kHz
200, 8	1.48 kHz	7 kHz	30 kHz
250, 12	800 Hz	6 kHz	11 kHz
300, 12	485 Hz	5.7 kHz	42 kHz

Actuators of the same overall length had roughly the same frequency characteristics, although they varied upwards with decreasing flexure length. The frequency values at ½ and zero deflection are less exact, as it was difficult to determine these deflections visually. Above the "zero deflection" frequency the actuator remains at roughly 2/3 deflection, for the 50% square wave signal used. Above that frequency the deflection can be set by adjusting the peak voltage or the pulse width. This characteristic is due to the inability of the hot arm to cool between cycles, so it averages the input power pulses [4]. The actuators were capable of higher frequency operation when loaded. For example, a 200 μm long actuator under a load of 7 μN had a maximum frequency of 2.5 kHz, although a mutual resonance with the force test beam led to chaotic deflections at some frequencies.

These actuators are intended for use in applications where they are not operated continuously, i.e. for positioning mechanisms, self-assembly, etc. However, a few of the actuators and arrays were operated for a large number of cycles to determine if this mode of operation would degrade their performance. The loaded actuator mentioned in the previous paragraph was operated for 980 million cycles at 2 kHz. At the end of the test the actuator was still reaching its full deflection, although it had eroded a 0.5 μm divot into the force test beam where it struck (refer to Fig. 2), which occasionally trapped the actuator tip. The actuator still reached full deflection, but had acquired a slight bow in the hot arm. Power consumption decreased 6% as the resistance of the device decreased over time. This was probably due to annealing of the hot arm. All of the actuators exhibited a 5-10% decrease in cold resistance after being operated for 10 seconds at nearly their maximum voltage.

These tests were conducted in an open bay lab and a condensate, probably water, collected in beads around the flexure and underneath the hot arm of some of the array actuators. For some tests this caused the array mechanism to stick down eventually, although the hot arms kept bowing with the drive signal. One array that did not stick down was operated for 54.5 million cycles at 800 Hz with no change in operation. The array was delivering a force of 18.2 μN to a test beam at an input power of 41 mW.

ACTUATOR ARRAY TESTS

The following sections report results of test performed on 2 to 12 actuators connected into arrays by four different mechanisms. For the arrays tested, space constraints made it necessary to choose a single actuator geometry and apply it to all the array types. The actuator chosen was 200 μm long, with a hot arm width of 2 μm, gap of 1.5 μm, and a flexure 50 μm long. Based on the single actuator test results, these

actuators have the best input power versus force characteristics for their length.

The four types of arrays were named for their connection schemes: flexural, pin-slot, rotating joint, and cascaded pushers. Close-up views of these four styles of array linkages are shown in Fig. 5a-d. The flexural yoke (Fig. 5a) is the original style, used successfully in the past [3]. The actuators are attached with flexures to a common yoke. Advantages are that yoke is compact, can be fabricated in a single releasable layer, and can have actuators attached from both sides. The disadvantage is that some force is lost in bending the flexures, and to decrease that loss the flexures must be made longer, taking up more area and making the structure less rigid.

The pin-slot type was an attempt to remedy the force lost in the flexural yoke. This works, and motors using this style of array were successfully operated, but has the disadvantage that the yoke is supported by dimples instead of the actuators. In testing this led to stick/slip motion and these arrays were the first to fail from stiction. Also, the yoke is free to rock and the actuator pins can slip out of it, even with a poly-3 cover to capture the pins.

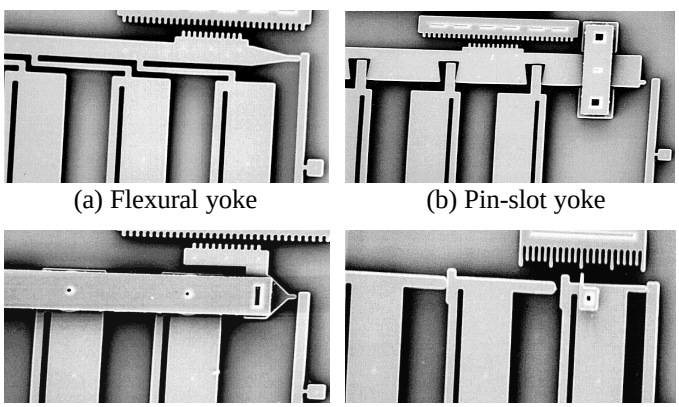

(a) Flexural yoke (b) Pin-slot yoke

(c) Rotary joint yoke (d) Cascaded pushers

Figure 5. Four variations on the actuator array concept. Each array is instrumented with force test beams and deflection scales which are also visible in these pictures.

The rotary joint type was by far the most successful, delivering the most force per input power to the test beams in all cases. It also has the advantage of being compact. Very little deflection is lost in the play of the rotary joints, and the yoke is supported primarily by the actuators instead of dimples. However, this design relies on the flanged hub capability of the SUMMiT process, or it would require three releasable poly layers if made in another process.

The cascaded pusher approach was also successful at eliminating force losses, but only at smaller deflections and in smaller arrays. This is because actuators farther back from the force application point must bend more before contacting the preceding actuator, so this is not practical for large arrays. Also, when these arrays are used in a back-bending mode, not all of the actuators will backbend the same amount, leaving gaps in the chain. This design can be used in a single releasable layer, and works for low deflection applications.

In general, each actuator consumes some power just bending itself, so for the lowest power consumption it is always best to use the fewest number of actuators that can deliver the required force and deflection. Figure 6 shows the force versus power for the four types of arrays with 8 actuators. Unfortunately the force of the arrays was underestimated when choosing the test beams, so the force available from the arrays could not be determined.

EXAMPLE APPLICATION

As an example of how these actuator arrays might be used, a rotary stepper motor was built which drives a multi-layer gear train, shown in Fig. 7. The gears step up RPM to drive a centrifugal blower, which is not shown because it has a layout flaw. Since the motor was designed without prior knowledge of the maximum possible array deflection in the SUMMiT process, a stacked drive gear was used to match the possibly small actuator array deflection to the standard Sandia gear tooth pitch. As a result of this study, it will be possible to design arrays that can drive the larger teeth directly.

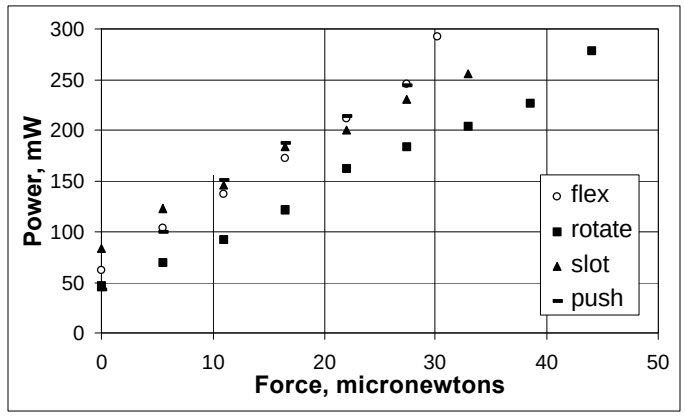

Figure 6. Force versus input power for four types of arrays with 8 actuators in each.

Figure 7. Rotary stepper motor. Main two-level gear adapts thermal actuator stroke to tooth pitch of standard, software-generated Sandia gears. Upper gear is planarized Poly-3.

ACKNOWLEDGEMENT

The portion of this work done at Sandia National Labs was supported by the U.S. Dept. of Energy under contract DE-AC04-94AL85000. Sandia is a multiprogram laboratory operated by Sandia Corporation, a Lockheed Martin Company, for the U.S. Dept. of Energy.

REFERENCES

[1] R. Nasby, J. Sneigowski, J. Smith, S. Montague, C. Barron, W. Eaton and P. McWhorter, *Solid State Sensors and Actuators Workshop* '96, Hilton Head SC, pp. 48-53.

[2] H. Guckel, J. Klein, T. Christenson, K. Skrobis, M. Laudon, and E. G. Lovell,, *Solid State Sensors and Actuators Workshop* '92, Hilton Head SC, pp. 73-75.

[3] J. Comtois and V. Bright, *Solid State Sensors and Actuators Workshop* '96, Hilton Head SC, pp. 174-177.

[4] J. Comtois, V. Bright, and M. Phipps, SPIE '95 vol. 2639, pp. 211-222.

[5] Sandia National Laboratories Web Page: http://www.mdl.sandia.gov